Optical propagation through non-Kolmogorov turbulence

Hua TANG and BaoLin OU

Citation: SCIENCE CHINA Information Sciences **56**, 042307 (2013); doi: 10.1007/s11432-011-4521-3

View online: https://engine.scichina.com/doi/10.1007/s11432-011-4521-3

View Table of Contents: https://engine.scichina.com/publisher/scp/journal/SCIS/56/4

Published by the Science China Press

SCIENCE CHINA
Information Sciences

• RESEARCH PAPER •

April 2013, Vol. 56 042307:1–042307:6
doi: 10.1007/s11432-011-4521-3

Optical propagation through non-Kolmogorov turbulence

TANG Hua* & OU BaoLin

School of Electronic and Information Engineering, Beihang University, Beijing 100191*, China*

Received September 9, 2010; accepted August 30, 2011; published online April 5, 2012

Abstract In this paper, the effects of the generalized exponent, the height and the zenith angle on the log-amplitude variance in the weak fluctuation are investigated. The theoretical results indicate that for the downlink, the log-amplitude variance of the Kolmogorov model is always smaller than that of the three-layer model, while for the uplink, there is a point of intersection in the log-amplitude variance curves of the two models. The different phenomena for the downlink and uplink are analyzed in detail. Further, we find a method to ascertain precise values of the boundary layer altitudes for the three-layer model under various atmospheric conditions through the analysis for the point of intersection. And at the point of intersection, the Kolmogorov model can be used to replace the three-layer model to simplify the analysis of the system performance. Moreover, the log-amplitude variance increases with the increase of the zenith angle.

Keywords atmospheric turbulence, three-layer model, log-amplitude variance, power spectral density, generalized exponent

Citation Tang H, Ou B L. Optical propagation through non-Kolmogorov turbulence. Sci China Inf Sci, 2013, 56: 042307(6), doi: 10.1007/s11432-011-4521-3

1 Introduction

For a long time, the Kolmogorov model has been widely used to describe the optical propagation through atmospheric turbulence, and is also used to calculate the free-space optical communication (FSO) system performance that is limited by atmospheric turbulence. However, recently experimental results indicate that the characteristics of the turbulence in the tropopause and stratosphere show great deviations from the predictions of the Kolmogorov model [1–3]. It can be understood by the fact that some anomalous behaviors [4–7] occur when the atmosphere is extremely stable, i.e., in this case the turbulence is no longer homogeneous in the three dimensions since the vertical component is suppressed. As a result, the Kolmogorov model will not be applicable. Besides, the Kolmogorov model is valid only in the inertial subrange, which limits the applicable scope of the Kolmogorov model in measuring FSO system performance.

Therefore, it is necessary to find other models more general than the Kolmogorov model to describe the turbulence. A generalized model called non-Kolmogorov model is presented in [8,9], which reduces to the Kolmogorov model with the generalized exponent $\alpha = 11/3$. And α is assumed to be any value in the range from 3 to 5. Further, experimental results in the tropopause, the stratosphere and even the free troposphere show that the parameters measuring FSO system performance, such as the scintillation index,

*Corresponding author (email: huatang@buaa.edu.cn)

deviate from the predictions based on the Kolmogorov model and the deviation has great dependence on the altitude. Therefore, a three-layer model [10] is presented, where α is the function of the height. The effects of the generalized exponent α and the height on the log-amplitude variance are presented [10–12]. However, the different phenomena for the downlink and uplink are not analyzed. And the analysis for the different phenomena can help deeply understand the essence of turbulent effects on FSO system performance and is useful for satellite communications.

In this paper, the effects of the generalized exponent α and the height on the log-amplitude variance are studied. The theoretical results indicate that for the downlink, the log-amplitude variance of the Kolmogorov model is always smaller than that of the three-layer model, while for the uplink, there is a point of intersection in the log-amplitude variance curves of the two models. The different phenomena for the downlink and uplink are analyzed in detail. Moreover, the log-amplitude variance increases with the increase of the zenith angle.

2 Kolmogorov spectrum and non-Kolmogorov spectrum

The basic power spectral density for the Kolmogorov model is defined as [11]

$$\phi_n(K) = 0.033 C_n^2 K^{-11/3}, \quad 2\pi/L_0 < K < 2\pi/l_0, \tag{1}$$

where C_n^2 is the refractive-index structure parameter, K is the magnitude of three dimensional wave number vector, l_0 and L_0 are the inner scale and outer scale of turbulence, respectively. The validity of the Kolmogorov spectrum is restricted to the inertial sub-range. The spectrum used to describe the non-Kolmogorov turbulence is defined as [11–13]

$$\phi_n(K, \alpha, h) = A(\alpha)\beta(h)K^{-\alpha}, \quad K > 0, \quad 3 < \alpha < 5, \tag{2}$$

where α is the generalized exponent, $A(\alpha)$ is the generalized amplitude, h is the vertical distance along the propagation path and $\beta(h)$ is the generalized refractive-index structure parameter with units of $\mathrm{m}^{3-\alpha}$, where

$$\beta(h) = A(11/3)/A(\alpha) \cdot C_n^2(h) \cdot (k/h)^{(\alpha/2-11/6)}$$

and $A(\alpha) = 2^{\alpha-6}(\alpha^2-5\alpha+6)\pi^{-3/2} \cdot \Gamma(\alpha/2-1)/\Gamma[(5-\alpha)/2]$ with $3 < \alpha < 5$, the wave number $k = 2\pi/\lambda$ and the gamma function $\Gamma(x)$.

3 The three-layer model

For α being in the range of 3 to 5, $\alpha(h)$ is expressed as [10,12]

$$\alpha(h) = \frac{\alpha_1}{1+(h/H_1)^{b_1}} + \frac{\alpha_2 \cdot (h/H_1)^{b_1}}{1+(h/H_1)^{b_1}} \cdot \frac{1}{1+(h/H_2)^{b_2}} + \frac{\alpha_3 \cdot (h/H_2)^{b_2}}{1+(h/H_2)^{b_2}}, \tag{3}$$

where $\alpha_1 = 11/3$, $\alpha_2 = 10/3$ and $\alpha_3 = 5$. H_1 and H_2 are the boundary layer altitudes and b_1 and b_2 are numerical coefficients of the model which need to be selected sufficiently to describe the flatness between layers. Figure 1 plots the generalized exponent α as the function of h for two sets of different values of the parameters b_1 and b_2 by taking $H_1 = 2$ km and $H_2 = 10$ km. Generally, the parameters H_1 and H_2 are in the regions of 1.5 to 3 km and 8 to 11 km, respectively. As shown in Figure 1, the atmosphere can be divided into three different zones: the boundary of the first one is up to about 2 km depicted by the Kolmogorov turbulence ($\alpha = 11/3$); the second one is the free troposphere up to about 10 km depicted by the helical turbulence ($\alpha = 10/3$); the third one is above the altitude of the free troposphere, i.e., the tropopause and the stratosphere ($\alpha = 5$); Thus it is called the three-layer model.

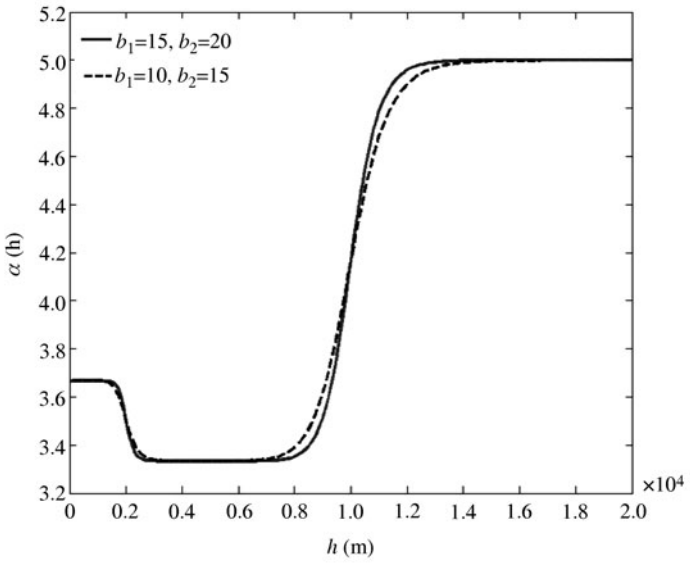

Figure 1 The generalized exponent α as the function of h for different b_1 and b_2 with H_1 =2 km, H_2 =10 km, $b_1 = 15$, $b_2 = 20$ for the solid line and $b_1 = 10$, $b_2 = 15$ for the dashed line.

4 Analysis and discussion

Following the same procedure discussed for the optical propagation in Kolmogorov turbulence, the log-amplitude variance σ_x^2 for the optical propagation in non-Kolmogorov turbulence for the downlink and uplink can be expressed as [12]

$$\sigma_x^2 = 0.033 \cdot k^{\frac{7}{6}} \int_0^H C_n^2(h) \cdot B(\alpha)[\sec(\zeta)]^{\frac{\alpha}{2}} h^{\frac{5}{6}} \mathrm{d}h, \quad 3 < \alpha < 5, \tag{4}$$

and

$$\sigma_x^2 = 0.033 \cdot k^{\frac{7}{6}} \int_0^H C_n^2(h) \cdot B(\alpha)[\sec(\zeta)]^{\frac{\alpha}{2}} \left(1 - \frac{h}{H}\right)^{\frac{\alpha-2}{2}} h^{\frac{5}{6}} \mathrm{d}h, \quad 3 < \alpha < 5, \tag{5}$$

where using the HV-21 model [14] for C_n^2, ζ is the zenith angle, H is the height of the transmitter for the downlink or the height of the receiver for the uplink and $B(\alpha) = -\pi^3/[2\Gamma(\alpha/2)\cos(\pi\alpha/4)]$.

The effects of α, H and ζ on the log-amplitude variance σ_x^2 for the downlink and uplink are investigated in Figures 2–4, where the parameter $\lambda = 1550$ nm is kept fixed. As shown in Figure 2, σ_x^2 for the downlink is larger than that for the uplink, as can be understood by the fact that σ_x^2 mainly results from the turbulence close to the receiver. And the turbulence close to the receiver for the downlink is stronger than that for the uplink since the strength of the turbulence decreases with the increase of the altitude according to the HV-21 model. Besides, with the increase of α, σ_x^2 decreases initially, and then increases when α is close to 5, as can be understood by the fact that when α is close to 3, the effect of the small-scale turbulence increases and the amplitude is mainly influenced by the small-scale turbulence, which results in a larger σ_x^2. While, as α is close to 5, the turbulence is anisotropic and the velocity field and the passive scalar (the temperature or the refractive index) field become independent, which results in an increase in σ_x^2. And the increase of σ_x^2 for the downlink is larger than that for the uplink since the effect of the turbulence on the downlink is larger than that on the uplink.

Figure 3 plots the log-amplitude variance σ_x^2 as the function of the height H for the downlink and uplink. As shown in Figure 3(a), for the uplink, there is a point of intersection in the σ_x^2 curves of the Kolmogorov model and the three-layer model, which is due to the different values of α in the two models and the effects of the anisotropic turbulence. However, Ref. [11] shows that for the uplink, the three-layer model induces larger losses than the Kolmogorov model, where the height of the receiver H is 8 km. However, in fact, with the increase of H, the three-layer model doesn't always induce larger losses

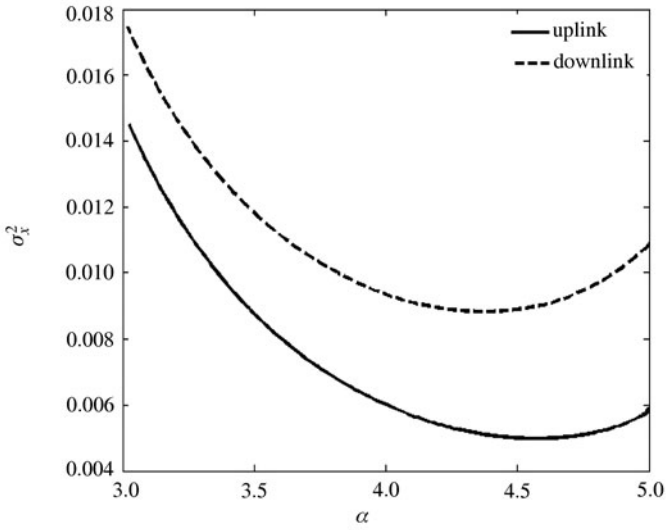

Figure 2 The log-amplitude variance σ_x^2 as the function of α for the downlink and uplink in the non-Kolmogorov model with $\zeta = 0$ rad and $H = 20$ km.

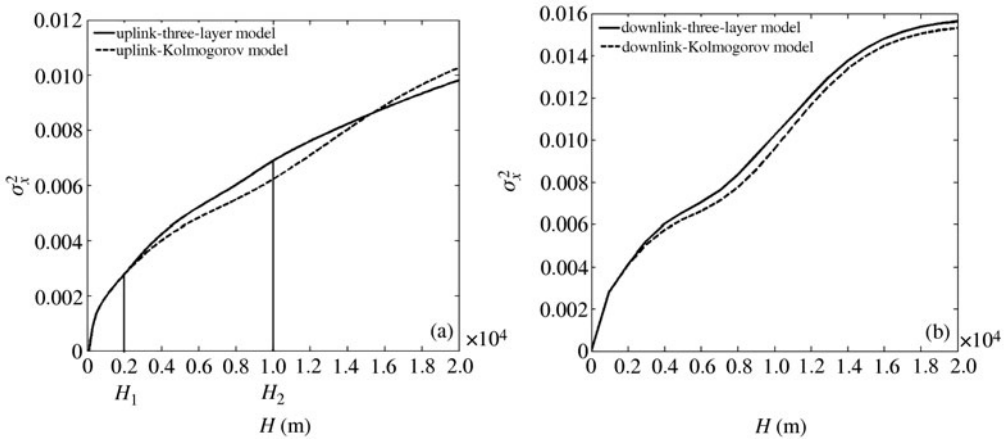

Figure 3 The log-amplitude variance as the function of the height H for the uplink (a) and downlink (b) in the Kolmogorov model and the three-layer model with $b_1 = 15$, $b_2 = 20$ and $\zeta = 0$ rad.

than the Kolmogorov model, that is to say, there is a height of the receiver at which the losses of the two models are equal.

To be specific, for the Kolmogorov model, α is set to 11/3 and for the three-layer model, α is assumed to be 11/3, 10/3 and 5 for different layers, respectively. When the height of the receiver H is no more than H_1, α in the Kolmogorov model and the three-layer model are equal, which makes σ_x^2 of the two models equal. And for H in the range from H_1 to H_2, when the variable of integration h in Eq. (5) is in the range of H_1 to H, for the three-layer model $\alpha = 10/3$ and for the Kolmogorov model $\alpha = 11/3$. As shown in Figure 2, for the uplink, σ_x^2 of $\alpha = 10/3$ is larger than that of $\alpha = 11/3$. Thus, in this case, σ_x^2 of the three-layer model is larger than that of the Kolmogorov model and the difference between them increases with the increase of H by the accumulated effects of the integration. Moreover, for H larger than H_2, when the variable of integration h in Eq. (5) is in the range of H_2 to H, for the three-layer model $\alpha = 5$ and for the Kolmogorov model $\alpha = 11/3$. As shown in Figure 2, for the uplink, σ_x^2 of $\alpha = 5$ is smaller than that of $\alpha = 11/3$, which makes the difference between σ_x^2 of the Kolmogorov model and that of the three-layer model gradually decrease by the accumulated effects of the integration. Thus there is a point of intersection in the σ_x^2 curves of the Kolmogorov model and the three-layer model at a height of the receiver H above the altitude H_2.

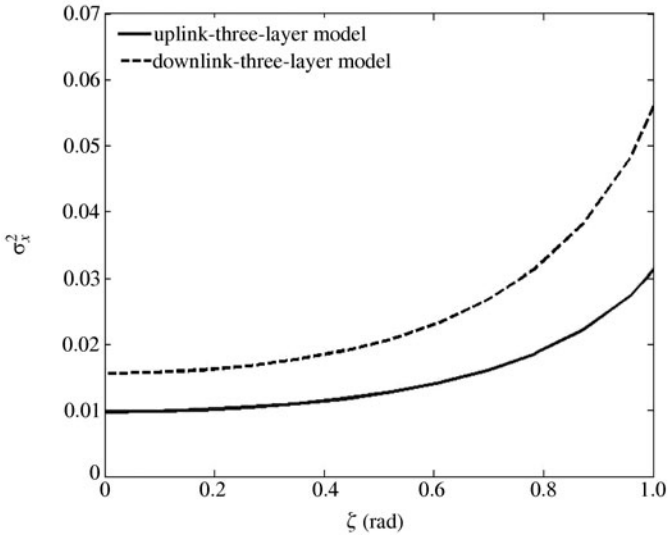

Figure 4 The log-amplitude variance as the function of the zenith angle ζ for the downlink and uplink in the three-layer model with $b_1 = 15$, $b_2 = 20$ and $H = 20$ km.

According to the analysis above, H_1 is the boundary altitude, below which σ_x^2 of the Kolmogorov model and the three-layer model are equal. And for H in the range of H_1 to $H_{\rm in}$ ($H_{\rm in}$ is the value of the altitude at the point of intersection), when $H = H_2$, the difference between σ_x^2 of the three-layer model and that of the Kolmogorov model is maximum. Therefore, we can ascertain the precise values of the parameters H_1 and H_2 for the three-layer model in various atmospheric conditions through comparing the calculation results of the Kolmogorov model with the measured results in the real atmosphere.

As h is no more than H_2, the analysis of σ_x^2 for the downlink is the same as that for the uplink. While, as h is more than H_2, the anisotropic turbulence has a larger effect on σ_x^2 for the downlink than that for the uplink, as shown in Figure 2, which makes σ_x^2 of $\alpha = 5$ larger than that of $\alpha = 11/3$. Therefore, σ_x^2 of the three-layer model is always larger than that of the Kolmogorov model, as shown in Figure 3(b).

Further, the length of the propagation path L satisfies $L = H\sec(\zeta)$. Thus, for the same height H, a larger zenith angle ζ corresponds to a longer propagation path. As a result, the log-amplitude variance σ_x^2 increases with the increase of ζ, as shown in Figure 4.

5 Conclusions

In conclusion, the effects of the generalized exponent α, the height H and the zenith angle ζ on the log-amplitude variance σ_x^2 are investigated for the downlink and uplink. The theoretical results indicate that for the uplink, there is a point of intersection in the σ_x^2 curves of the Kolmogorov model and the three-layer model, which is attributed to the different values of α in the two models and the effect of the anisotropic turbulence. While for the downlink, σ_x^2 of the Kolmogorov model is always smaller than that of the three-layer model since the strongly anisotropic turbulence in the stratosphere results in a larger σ_x^2 than the uplink, which makes σ_x^2 of $\alpha = 5$ larger than that of $\alpha = 11/3$, as shown in Figure 2. Further, according to the analysis for the point of intersection, we can compare the calculation results of the Kolmogorov model with the measured results in the real atmosphere and ascertain the precise values of H_1 and H_2 for the three-layer model in various atmospheric conditions through the differences between the two results. And at the point of intersection, the Kolmogorov model can be used to replace the three-layer model to simplify the analysis of the system. Moreover, the log-amplitude variance σ_x^2 increases with the increase of the zenith angle ζ.

Acknowledgements

This work was supported by Key Project of National Natural Science Foundation of China (Grant No. 60837004), Project of National Natural Science Foundation of China (Grant No. 61101005), Project-sponsored by SRF for ROCS, SEM, Fundamental Research Funds for the Central Universities (Grant No. YWF-11-03-Q-159).

References

1 Rao C H, Jiang W H, Ling N. Atmospheric characterization with Shack-Hartmann wave-front sensors for non-Kolmogorov turbulence. Opt Eng, 2002, 41: 534–541
2 Zilberman A, Golbraikh E, Kopeika N S, et al. Lidar study of aerosol turbulence characteristics in the troposphere: Kolmogorov and non-Kolmogorov turbulence. Atmos Res, 2008, 88: 66–77
3 Kyrazis D T, Wissler J B, Keating D D B, et al. Measurement of optical turbulence in the upper troposphere and lower stratosphere. P SPIE, 1994, 2120: 43–55
4 Dayton D, Pierson B, Spielbusch B, et al. Atmospheric structure function measurements with a Shack-Hartmann wave front sensor. Opt Lett, 1992, 17: 1737–1739
5 Rao C H, Jiang W H, Ling N. Measuring the power-law exponent of an atmospheric turbulence phase power spectrum with a Shack Hartmann wave-front sensor. Opt Lett, 1999, 24: 1008–1010
6 Belen'kii M S. Effect of the stratosphere on star image motion. Opt Lett, 1995, 20: 1359–1361
7 Belen'kii M S, Karis S J, Osmon C L, et al. Experimental evidence of the effects of non-Kolmogorov turbulence and anisotropy of turbulence. P SPIE, 1999, 3749: 50–51
8 Beland R R. Some aspects of propagation through weak isotropic non-Kolmogorov turbulence. P SPIE, 1995, 2375: 6–16
9 Toselli I, Andrews L C, Phillips R L, et al. Free space optical system performance for laser beam propagation through non Kolmogorov turbulence for uplink and downlink paths. P SPIE, 2007, 6708: 670803
10 Zilberman A, Golbraikh E, Kopeika N S. Propagation of electromagnetic waves in Kolmogorov and non-Kolmogorov atmospheric turbulence: three-layer altitude model. Appl Opt, 2008, 47: 6385–6391
11 Zilberman A, Golbraikh E, Kopeika N S. Some limitations on optical communication reliability through Kolmogorov and non-Kolmogorov turbulence. Opt Commun, 2010, 283: 1229–1235
12 Kopeika N S, Zilberman A, Golbraikh E. Imaging and communications through non-Kolmogorov turbulence. P SPIE, 2009, 7463: 746307
13 Tan L Y, Du W H, Ma J, et al. Log-amplitude variance for a Gaussian-beam wave propagating through non-Kolmogorov turbulence. Opt Express, 2010, 18: 451–462
14 Majumdar A K, Ricklin J C. Effects of the atmospheric channel on free-space laser communications. P SPIE, 2005, 5892: 58920K